



The transport of atmospheric NO_x and HNO₃ over Cape Town

B. J. Abiodun¹, A. M. Ojumu², S. Jenner¹, and T. V. Ojumu³

¹Climate Systems Analysis Group, Department of Environmental and Geographical Science, University of Cape Town, South Africa

²Department of Environmental and Agricultural Sciences, University of South Africa, South Africa

³Department of Chemical Engineering, Cape Peninsula University of Technology, South Africa

Correspondence to: B. J. Abiodun (babiodun@csag.uct.ac.za)

Received: 5 March 2013 – Published in Atmos. Chem. Phys. Discuss.: 3 May 2013

Revised: 29 August 2013 – Accepted: 3 December 2013 – Published: 20 January 2014

Abstract. Cape Town, the most popular tourist city in Africa, usually experiences air pollution with unpleasant odour in winter. Previous studies have associated the pollution with local emission of pollutants within the city. The present study examines the transport of atmospheric pollutants (NO_x and HNO₃) over South Africa and shows how the transport of pollutants from the Mpumalanga Highveld, a major South African industrial area, may contribute to the pollution in Cape Town. The study analysed observation data (2001–2008) from the Cape Town air-quality network and simulation data (2001–2004) from a regional climate model (RegCM) over southern Africa. The simulation accounts for the influence of complex topography, atmospheric conditions, and atmospheric chemistry on emission and transport of pollutants over southern Africa. Flux budget analysis was used to examine whether Cape Town is a source or sink for NO_x and HNO₃ during the extreme pollution events.

The results show that extreme pollution events in Cape Town are associated with the lower level (surface – 850 hPa) transport of NO_x from the Mpumalanga Highveld to Cape Town, and with a tongue of high concentration of HNO₃ that extends from the Mpumalanga Highveld to Cape Town along the south coast of South Africa. The prevailing atmospheric conditions during the extreme pollution events feature an upper-level (700 hPa) anticyclone over South Africa and a lower-level col over Cape Town. The anticyclone induces a strong subsidence motion, which prevents vertical mixing of the pollutants and caps high concentration of pollutants close to the surface as they are transported from the Mpumalanga Highveld toward Cape Town. The col accumulates the pollutants over the city. This study shows that Cape Town can be a sink for the NO_x and HNO₃ during extreme

pollution events and suggests that the accumulation of pollutants transported from other areas (e.g. the Mpumalanga Highveld) may contribute to the air pollution in Cape Town.

1 Introduction

Accumulation of atmospheric mono-nitrogen oxides (NO_x) and its derivatives (i.e. HNO₃) may have severe impacts on climate, environment, and human health. For instance, reaction of NO_x and sulphur dioxide in the presence of moisture produces acid rain (Likens and Bormann, 1974; Wettburn, 1988), which corrodes cars (Schulz et al., 2000; Samie et al., 2007), buildings and historical monuments (Cheng et al., 1987; Schuster et al., 1994; Bravo et al., 2006) and makes streams and lakes acidic, hence uninhabitable for fish (Minns et al., 1986). Reaction of NO_x and ammonia with other substances generates particles and nitric acid (HNO₃). The particles have negative impacts on the human respiratory system, damage lung tissue, and cause premature death (Schwartz and Marcus, 1990; Ostro et al., 1991; Gaudermann et al., 2000). Small particles, in particular, can penetrate deeply into sensitive parts of the human lungs and cause respiratory diseases, such as emphysema and bronchitis (Yang and Omaye, 2009). They can also aggravate existing heart disease (Stern et al., 1988). Nitric acid, on the other hand, corrodes and degrades metals (Dean, 1990). Excess nitrate is harmful to ecosystems because it can lead to “eutrophication”, which deteriorates water quality and kills fish. However, the complexity of nutrient cycling in ecosystems may cause the long-term impact of nitric acid to take decades to become apparent (Fields, 2004). Reaction of NO_x with volatile organic

compounds (VOCs) in the presence of heat and sunlight produces ozone, a major component of smog. It is well known that smog and ozone cause nose and throat irritation, and eventually death. Ozone can also damage vegetation and reduce crop yields. Cape Town, Africa's most popular tourist city with about 3.5 million people (StatsSA, 2012), is usually covered with smog (called brown haze) in winter. Several studies (e.g. Wicking-Baird et al., 1997) have linked the brown haze to unpleasant odours, health effects and visibility impairment in the city.

A combination of geographical and meteorological factors makes Cape Town favourable for the accumulation of air pollutants. The location of Cape Town (33.9° S, 18.4° E) at the southwestern tip of Africa (Fig. 1) influences the wind patterns which it experiences. The city is bordered by the Table Mountain complex to the southwest, False Bay to the south, and Table Bay to the west. At this subtropical latitude, calm conditions are sometimes produced over the city under stagnant anticyclonic flows. The subsidence temperature inversion suppresses vertical exchange of air and pollutants during most periods of the year. In addition, radiative cooling at night produces a stable layer at the surface to form surface inversion, which prevents the vertical dispersion of pollutants during the early mornings. The South Atlantic anti-cyclone and the cold Benguela Current induce surface inversion, which strengthens over the Cape Town (Preston-Whyte et al., 1977). Owing to the temperature contrast between the cold Benguela Current and the warm land, sea breezes develop during the day and this traps pollutants within the Cape Town basin. Berg winds, which occur when a high-pressure system over Kwazulu-Natal is associated with a high-pressure system over the Western Cape with an approaching cold front, favour brown haze episodes, because the warm northeasterly reduces dew-point temperature during the night (Jury et al., 1990). Consequently, extreme high-pollution events occur from April to September; and, whenever the brown haze occurs during this period, it extends over most of Cape Town and shifts according to the prevailing wind direction (Wicking-Baird et al., 1997).

Many studies have investigated pollution over Cape Town, but their focus has been on the influence of locally emitted pollutants. Wicking-Baird et al. (1997) showed that vehicles are the principal source of pollution in Cape Town, accounting for about 65% of the brown haze. Local emitting industries also contribute considerably, accounting for about 22% of the brown haze. The use of wood for fires by a large sector of the population accounts for about 11% of the brown haze, and natural sources, such as wind-blown dust and sea salt, contribute about 2 % towards the brown haze. Walton (2005) identified the Caltex Oil Refinery and Consol Glass as the two main sources of pollution in the city, while the Cape Town Central Business District, Cape Town International Airport, and townships of Khayelitsha and Mitchell's Plain are also major sources. However, none of these previous studies accounted for the contribution of pollutants trans-

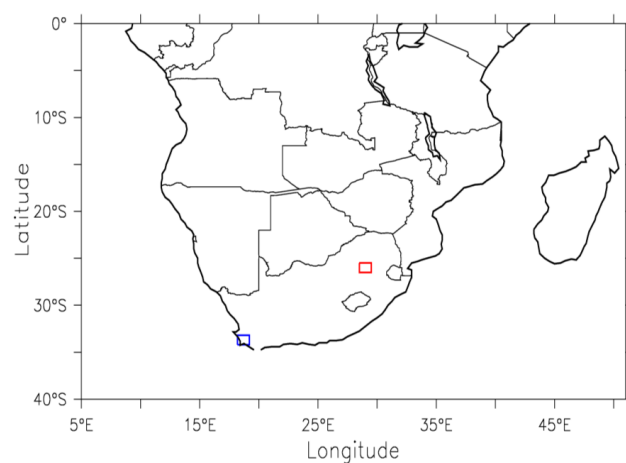


Fig. 1. Map of southern Africa showing the Cape Town area (blue box) at the southwestern tip of South Africa and the Mpumalanga Highveld (red box), the most industrialised area in South Africa, in the northeastern part of South Africa.

ported from remote sources to Cape Town. Since secondary pollutants like HNO₃ can be transported by wind to cause health impacts far from their original sources, it is important to investigate how pollutants transported from remote sources in South Africa can contribute to the air-quality problem in Cape Town. This paper addresses how NO_x and HNO₃ transported from the Mpumalanga Highveld (the most industrialised region in South Africa) can accumulate over Cape Town.

The Mpumalanga Highveld accounts for 90 % of South Africa's emission of nitrogen oxides and other gases (Collett et al., 2010). Previous studies (Freiman and Piketh, 2003; Piketh et al., 2002) have considered regional scale transport and recirculation of pollutants emitted from the Highveld (using trajectory models with reanalysis data with low resolution) and showed that most of the pollutants from the Highveld are transported to the Indian Ocean by the westerlies, at 700 hPa.

However, since the Mpumalanga Highveld is located northeast of Cape Town, a persistent low-level, northeasterly flow over South Africa can transport the pollutants from the Highveld to Cape Town. Such a transport has not been captured by previous studies, which used low resolution atmospheric data in trajectory models. In addition, trajectory models cannot account for chemical reactions that occur during the transport of air pollutants, making it difficult to account for the concentration of primary and secondary pollutants separately. Meanwhile, in some cases, the concentration of the secondary pollutants may be higher than that of their precursors. In the present study, a high-resolution atmospheric-chemistry model that accounts for the influence of topography, atmospheric conditions, and chemical reactions among

the atmospheric gasses is used to investigate the transport of pollutants from the Mpumalanga Highveld to Cape Town.

NO_x concentration in the atmosphere is essentially the total concentration of nitric oxide (NO) and nitrogen dioxide (NO₂), while the acid derivate, nitric acid (HNO₃), is an oxidative product of NO_x, as shown in Reactions (R1)–(R4).



The ratio of NO to NO₂ is determined by ozone availability and sunshine (or temperature); and nitrous acid and nitric acid are produced by reaction of NO₂ with moisture/water Eq. (4). Nitrous acid is essentially dominant in heterogenous phase, while in gaseous phase condition, nitric acid dominates (Seinfeld and Pandis, 2006). Although production of NO_x from combustion of nitrogen is characterized by high activation energy, 320kcal/mol (Dean and Bozzelli, 2000), the sensitivity of the reaction to temperature is not only due to the high activation energy, but also to increasing concentration of oxygen atoms during the combustion. Most of the reactions in Reactions (R1)–(R4) proceed at fairly low activation energies, thus promoting abundant NO_x and/or acids in the atmosphere. For example, the activation temperature of Reaction (R1) is 210 K (Sander et al., 2011), indicating that the reaction is feasible even at sub-zero temperatures.

The aim of the present study is to examine the transport of NO_x and HNO₃ over South Africa and to investigate how pollutants from the Mpumalanga Highveld may contribute to air pollution in Cape Town. The study combines an analysis of station observations and regional climate model simulation to achieve the aim. It calculates the flux budget of the pollutants over Cape Town and investigates the atmospheric conditions that favour accumulation of pollutants over the city. The methodology used in the study is discussed in Sect. 2, results and discussions are in Sect. 3, while the conclusion is in Sect. 4.

2 Methodology

2.1 Observed data

This study used meteorological and pollution data from four stations within the Cape Town air-quality monitoring network (Fig. 2). The network comprises 12 stations within a 500 km² area and measures ambient concentrations of selected pollutants considered hazardous to human health and ecology (City of Cape Town, 2005), as well as relevant meteorological parameters that might explain high concentrations.

The stations with relevant observations for the period of the study are City Hall, Goodwood, Bothasig and Tableview (Fig. 2). Vehicular emissions are the prime source of

pollution for the City Hall station, which is located opposite the city's busy taxi rank, bus station and rail terminus. Goodwood is a mixed residential and commercial area with nearby industry to the southeast and southwest. The nearby national road, the N2, carries commuter traffic from Cape Town's northern suburbs to the City, and another busy national road, the N7, passes along the south side of this area. Road traffic near these two stations is congested during the morning and evening commute. Although located near arterial roads, Bothasig and Tableview stations experience less traffic-sourced pollution than the City Hall station, because the number of commuters on the arterial roads is lower.

The data used for this study comprises the hourly average of NO, NO₂ and NO_x concentrations, wind speed, wind direction, and temperature for 10 years (2000–2009). The data were analysed to identify temporal variation of concentrations and associated atmospheric conditions to the peaks. Diurnal variation was analysed to investigate the concentration peaks and the contribution of the atmospheric conditions. Monthly mean concentrations of pollutants and climatological variables were used to identify the influence of seasonal variation. Monthly temperature and rainfall data from the Climate Research Unit (CRU; Mitchell and Jones, 2005) were analysed to supplement the station data in validating the model simulation.

3 Model descriptions and set-ups

The study applied the International Centre for Theoretical Physics (ICTP) Regional Climate model (version 4) with chemistry (hereafter, RegCM) to simulate the climate and pollution transport over Southern Africa (Fig. 3a). The model allows online coupling of atmospheric and chemistry parameters. The climate component has been successfully tested over Southern Africa (Sylla et al., 2009). RegCM is a hydrostatic, sigma-coordinate model (Pal et al., 2007; Giorgi et al., 2012). The model has various options for physics and chemistry parameterisations. In the present study, the model used the CCM3 (Kiehl et al., 1996) radiation scheme for radiation calculations, the (Grell et al., 2005) mass-flux cumulus scheme with Fritsch and Chappell (1980) closure for convection, and the Holtslag and Boville (1993) scheme for planetary boundary-layer parameterisation.

Surface-layer, land–atmosphere interactions were represented with BATS1E (Biosphere-Atmosphere Transfer Scheme) (Dickinson et al., 1993), which is based on Monin–Obukhov similarity relations (Monin and Obukhov, 1954). For the chemistry routines, the photochemical Carbon Bond Mechanism-Z (CBM-Z) (Zaveri and Peters, 1999) was used. Photolysis is based on the Tropospheric Ultraviolet-Visible Model (TUV) scheme developed by Madronich and Flocke (1999). For dry deposition the model used the CLM4 (Community Land Model 4) developed after Wesley (1989), and wet deposition follows the MOZART global model



Fig. 2. Map of the Cape Town, showing the air quality network in Cape Town and the location of four observation stations (Bothasig, City Hall, Goodwood and Tableview) used in the study (source: <http://web1.capetown.gov.za/web1/cityairpol>). The colour code indicates different suburbs in the city.

(Emmons et al., 2010). Shalaby et al. (2012) presents a detailed description of the gas-phase chemistry in RegCM.

The RegCM simulation was set up with a 35km horizontal resolution. The simulation domain centres on 33° S and 24° E and extends, with the Lambert conformal projection, from 16.62° W to 54.41° E and from 10.5° S to 40.45° S (Fig. 3a). In the vertical, the domain spans 18 sigma levels, with highest resolution near the surface and lowest resolution near the model top. Initial and lateral boundary meteorological conditions were provided by ERA-Interim 1.5° × 1.5° gridded reanalysis data from ECMWF (European Centre for Medium-Range Weather Forecasts). The global emissions data sets (1° × 1° resolution) used in the simulation were derived from the Coupled Model Intercomparison Project Phase 5 (CMIP5) RCP (Representative Concentration Pathways, Moss et al., 2010; van Vuuren et al., 2011) emission, provided with the standard RegCM package (http://clima-dods.ictp.it/data/d8/cordex/RCP_EMGLOB_PROCESSED). The emissions data set has monthly variation; the horizontal distribution of NO emission over Southern Africa, averaged between 2001 and 2004, is shown in Fig. 3b, while the monthly

values over Mpumalanga and over Cape Town for this period are shown in Fig. 3c. The simulation covers a period of four years and three months (i.e. October 2000–December 2004). The first three months' simulations were discarded as model spin-up, while the remaining four years' simulations were analysed for the study.

3.1 Pollutants flux budget

Flux budget analysis was used to calculate the net flux of the pollutants (NO_x and HNO₃) over Cape Town and to examine whether the city is a source or sink for the pollutants. The pollutant net flux (F_{Net}) is defined as:

$$F_{\text{Net}} = (F_E - F_W) + (F_N - F_S) \quad (1)$$

where F_E , F_W , F_N , and F_S are the pollutant fluxes at the eastern, western, northern and southern boundaries of Cape Town (Fig. 1), respectively.

A positive zonal flux (F_E or F_W) implies a westerly pollutant flux (i.e. pollutant flux from the westerly direction), while a negative zonal flux means the opposite. A positive meridional flux (F_N or F_S) denotes a southerly pollutant flux (i.e. pollutant flux from the southerly direction), while a negative zonal flux means the opposite. A positive net flux indicates divergence of a pollutant over the city, meaning that the city is a net source for the pollutant. A negative net flux indicates convergence (or accumulation) of pollutants over the city, meaning that the city is a net sink for the pollutant.

4 Results and discussion

This section presents and discusses the results of the study in three parts. The first part describes the temporal (diurnal and seasonal) variation of the observed pollutant concentrations and meteorological variables at the four stations (City Hall, Goodwood, Bothasig and Tableview) within the city (see Fig. 2). The second part compares RegCM simulation (pollutant concentrations and meteorological variables) with the observed data. The third part discusses the characteristics of the simulated NO_x (NO and NO₂) and HNO₃ over Cape Town.

4.1 Observed nitrogen oxides and atmospheric conditions over Cape Town

4.1.1 Diurnal variation

The diurnal cycle of NO, NO₂, NO_x (Fig. 4) shows that the pollutants have the highest concentration at City Hall and the lowest concentration at Tableview. This is because City Hall is located in the heart of the city where the emission of NO from daily anthropogenic activity (traffic, industrial, business) is greatest. The diurnal variation of NO concentration (Fig. 4a) shows two peaks (morning and evening peaks) at City Hall, but one peak (in morning) at other stations

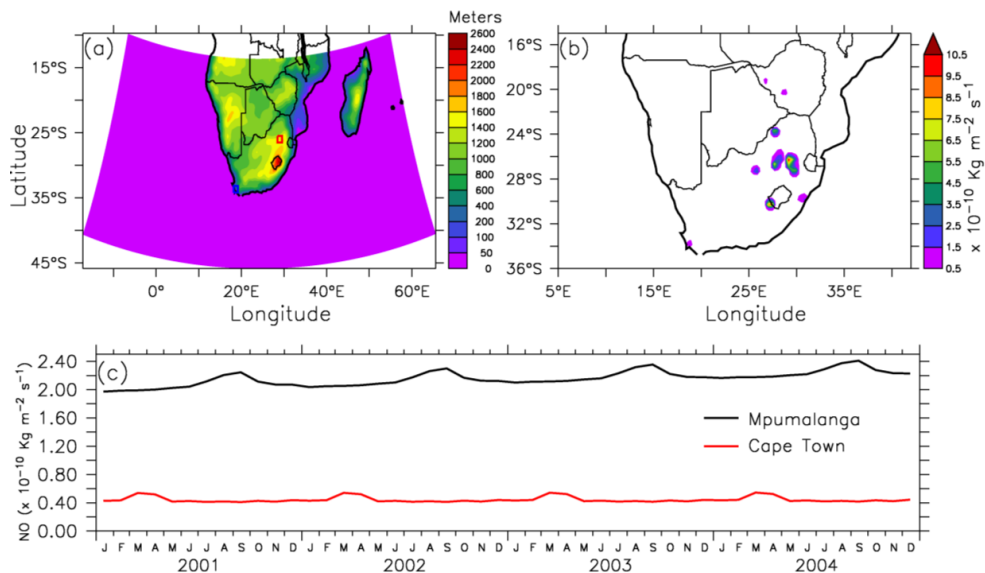


Fig. 3. (a) RegCM simulation domain indicating the topography (in metres) of southern Africa as seen by the model; (b) the annual mean of NO emission over South Africa used in the model; (c) the temporal variation of NO emission over Mpumalanga and Cape Town in 2001–2004.

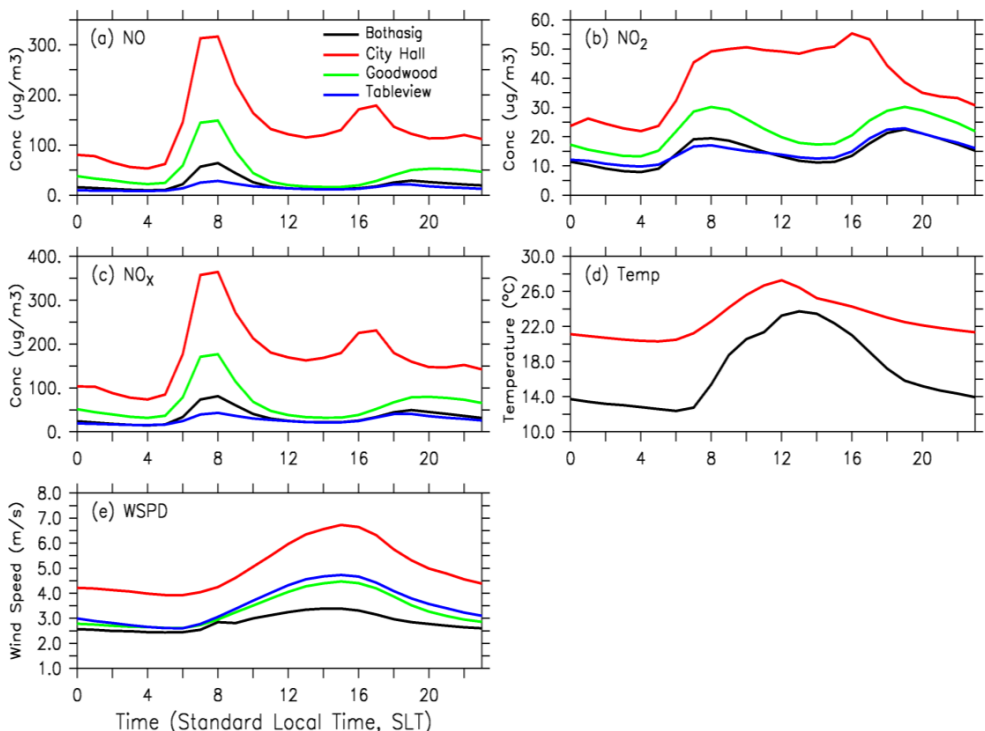


Fig. 4. Diurnal variation of observed (a) NO, (b) NO₂, (c) NO_x (d) temperature, and (e) wind speed at four monitoring stations in Cape Town. The values are for all seasons (2001–2008).

(Bothasig, Goodwood, and Tableview). The morning peaks (City Hall: $280 \mu\text{g m}^{-3}$; Goodwood: $120 \mu\text{g m}^{-3}$; Bothasig: $60 \mu\text{g m}^{-3}$; and Tableview: $20 \mu\text{g m}^{-3}$) occur at 08:00 SLT (Standard Local Time), while the evening peak (City Hall:

$60 \mu\text{g m}^{-3}$) occurs at 16:00 SLT. Although Bothasig, Goodwood, and Tableview show no evening peak, the NO concentration is higher in the evening (18:00–20:00 SLT) than in the afternoon.

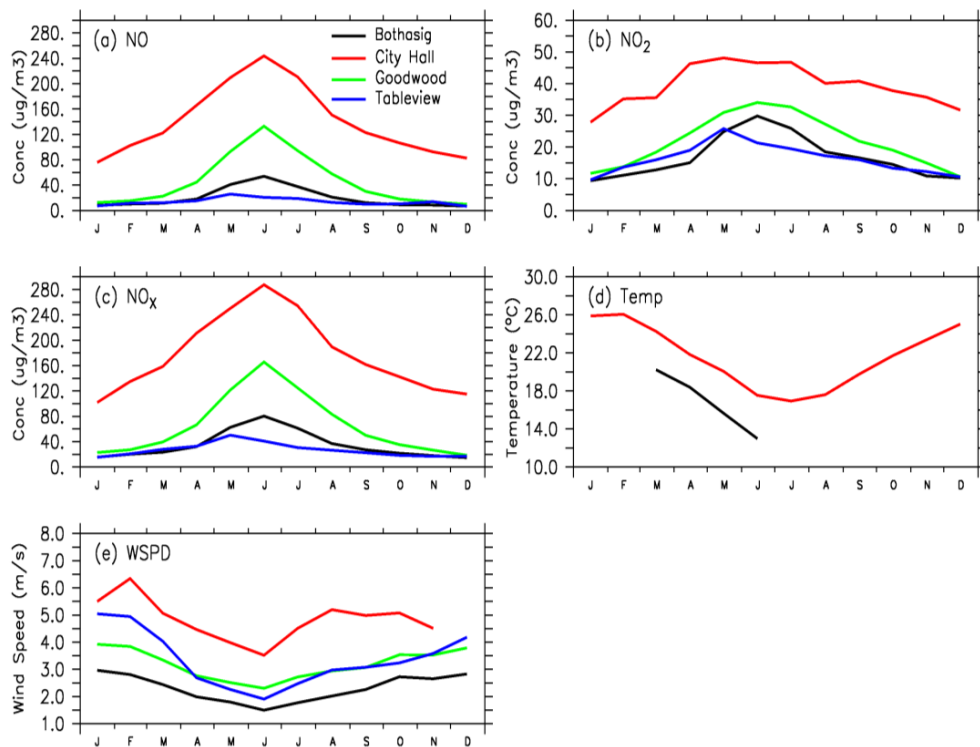


Fig. 5. The monthly mean of observed (a) NO, (b) NO₂, (c) NO_x, (d) Temperature, (e) wind speed, and (d) wind direction at four monitoring stations in Cape Town (2001–2008).

The morning peaks and the evening peak at City Hall can be attributed to the high commuter traffic in the city, because people rush to work and school in the morning (around 08:00 SLT) and return home in the evening (16:00 SLT). However, the concentration peak is higher in the morning than in the evening, because the traffic rush is greater in the morning than in the evening, as schools and offices open at same time in the morning (08:00 SLT) but close at different times in the afternoon.

The diurnal variation of NO₂ differs from that of NO. At City Hall, the diurnal variation of NO₂ shows no distinct peak; instead, it shows a uniform concentration (about 50 $\mu\text{g m}^{-3}$) during the day (08:00–18:00 SLT) and a lower concentration (about 20 $\mu\text{g m}^{-3}$) at night. In contrast, the diurnal variation of NO shows two distinct peaks at other stations (Goodwood: 25 $\mu\text{g m}^{-3}$; Tableview and Bothasig: 18 $\mu\text{g m}^{-3}$) in the morning (08:00 SLT) and in the evening (19:00 SLT). However, at all stations, the NO₂ concentration is smaller than that of NO, because NO_x are mainly emitted in the form of NO, which is later oxidized to NO₂ by different photochemical reactions (Eq. 1). The rate of these reactions depends on favourable atmospheric conditions. Nevertheless, since the magnitude of NO concentration is about five times higher than that of NO₂ (Fig. 4), the diurnal variation of NO_x (NO + NO₂) follows that of NO.

However, the diurnal variation of meteorological variables may also play an important role in the diurnal variation of the pollutants' concentration. The diurnal variation in wind speed (Fig. 4e) and surface temperature (Fig. 4d) may enhance the concentrations of the pollutants in the morning and lower them in the afternoon. For instance, the weak surface wind speed in the morning (Fig. 4b) may lead to the accumulation and higher concentration of NO, while the higher wind speed in the afternoon may reduce NO concentration.

Besides, in the morning, the surface inversion layer (induced by low surface temperature from the nocturnal radiative cooling) can inhibit vertical mixing of the NO. In the afternoon, the surface heating increases the surface temperature and the development of a mixing layer will erode the inversion layer. Hence, pollutants trapped below the surface layer will rise and disperse, reducing the NO concentration in the afternoon.

In contrast, the increase in NO₂ concentration in afternoon may be attributed to an increase in temperature which can enhance the generation of more NO₂ owing to chemical reaction (see Eq. 1). This could further explain why the NO₂ concentration is much higher at the City Hall (where maximum temperature is about 27°C) than at Bothasig (where the maximum temperature is about 22°C).

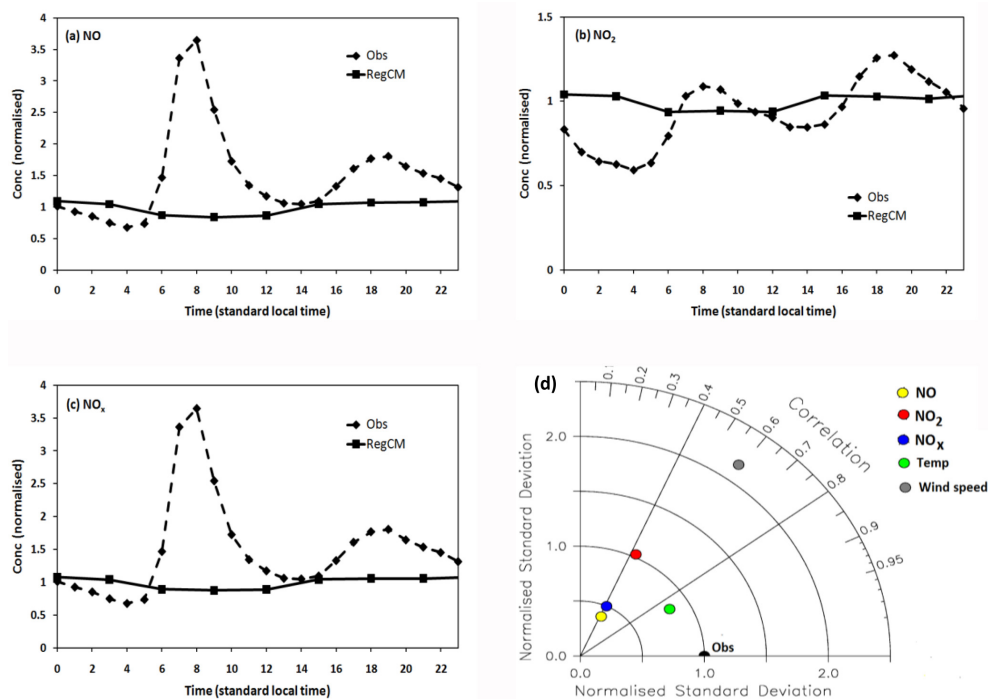


Fig. 6. Comparison of the simulated (RegCM) and observed diurnal variation of (a) NO, (b) NO₂, and (c) NO_x concentrations. (d) shows the Taylor diagram, which uses correlation coefficient and normalised standard deviation to compare variations in the simulated and observed (Obs) daily mean NO, NO₂, NO_x, temperature (Temp), and wind speed. The average observation over the four stations is indicated as Obs. The normalised standard deviations are obtained by dividing the simulated and observed standard deviations with the observed standard deviation.

4.1.2 Seasonal variation

The concentration of the pollutants also varies with seasons (Fig. 5). The seasonal variations of the atmospheric conditions may play a major role in the seasonal variation of the pollutants' concentration. At all stations, NO shows a maximum concentration (City Hall, $200 \mu\text{g m}^{-3}$; Goodwood, $100 \mu\text{g m}^{-3}$; Bothasig, $100 \mu\text{g m}^{-3}$; Tableview, $30 \mu\text{g m}^{-3}$) in early winter (June) and a minimum concentration (City Hall: $80 \mu\text{g m}^{-3}$; Goodwood, Bothasig and Tableview: $20 \mu\text{g m}^{-3}$) in summer (December–February). Nevertheless, the seasonal variation is most pronounced at City Hall and least defined at Tableview (Fig. 5a). The occurrence of maximum concentration of NO in winter can be attributed to the weak wind speed and low surface temperature during this period, as both conditions do not favour the pollutant dispersion and its conversion to NO₂ through the reaction in Eq. (1).

The seasonal variation of NO₂ (and NO_x) is similar to that of NO (Fig. 5), except that: (1) the concentration of NO₂ is smaller than that of NO; (2) at City Hall, the maximum concentration of NO₂ extends over more months (March–July) than that of NO; and (3) at Tableview, the maximum concentration of NO₂ is in March–May instead of in June (as for NO). The occurrence of maximum concentration of NO₂ in March–July can be attributed to a balance between NO con-

centration and atmospheric conditions that favour NO₂ production. For instance, less NO concentration limits the production of NO₂ in January (when the temperature is most favourable for the production), and less favourable atmospheric conditions prevent a peak concentration of NO₂ in June, when the NO concentration reaches its peak.

4.2 Model validation

The diurnal variation of the simulated pollutants (NO, NO₂ and NO_x) shows a weaker diurnal variation than the observed (Fig. 6). This is because the monthly emissions data used in simulation did not account for diurnal variation of the local sources (i.e. the high commuter traffic in the city) discussed earlier (see Sect. 3.1.1). The simulated diurnal variation shows the lowest concentration during the day (between 09:00 and 14:00 SLT), when the enhancement of boundary-layer vertical mixing reduces the pollutants' concentration at lower level. This is consistent with a decrease in the observed NO and NO_x concentration between 12:00 and 15:00 SLT.

The daily mean concentration of the simulated NO shows a weak correlation with the observed values, and the standard deviation is lower than the observed (Fig. 6). The correlation coefficient is about 0.4, and the normalised standard deviation (i.e. simulated standard deviation divided by the observed standard deviation) is 0.4. The simulated correlation

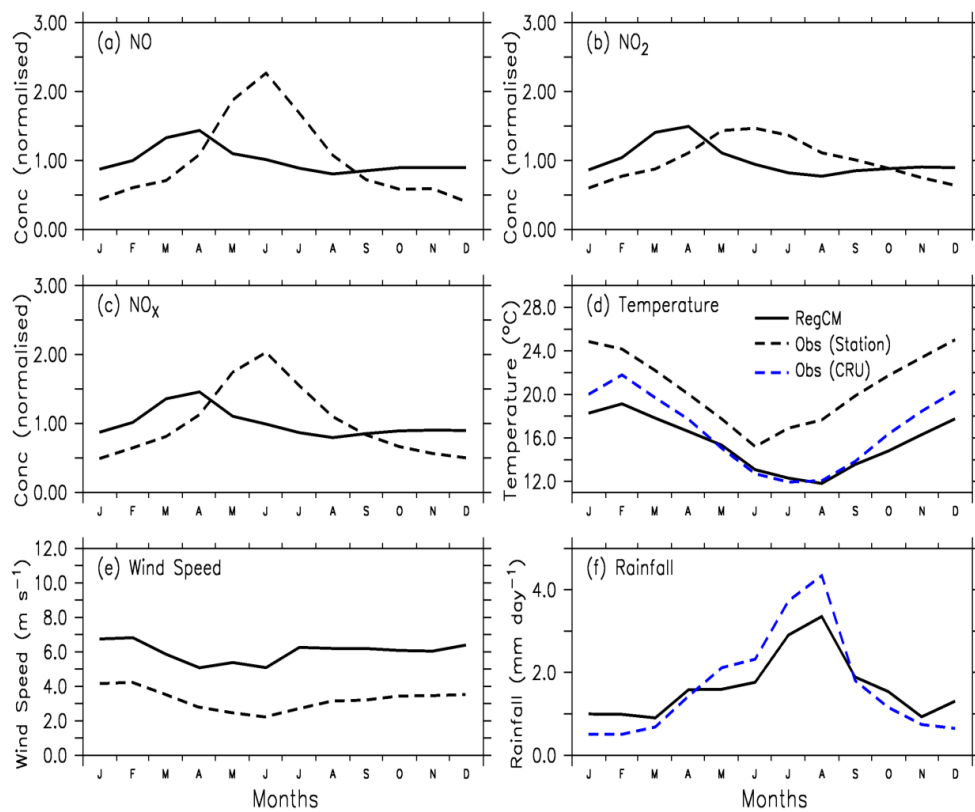


Fig. 7. Seasonal variation of observed and simulated (a) NO, (b) NO₂, (c) NO_x, (d) Temperature (°C), (e) Wind Speed (m s^{-1}), and (f) Rainfall (mm day^{-1}). The NO, NO₂ and NO_x concentration are normalised with their annual mean values. The average observation over the four stations is indicated as Obs (station).

between the observed and simulated NO₂ is also 0.4, but the normalized standard deviation (about 1.0) is much better than that of NO. The normalized standard deviation of NO_x (0.50; Fig. 6d) falls between those of NO and NO₂, but the correlation coefficient is also 0.4. There is a better correlation between the simulated and observed atmospheric variables than with the pollutants' concentrations, suggesting that the weak correlation between the observed and simulated pollutant concentration may be due to the RegCM chemistry. However, the RegCM shows its best performance in simulating temperature – the correlation coefficient is 0.85 and the normalized standard deviation is 0.8. The discrepancy between simulated pollutant and observation may be due to the low resolution of the simulation and low resolution of the emission data sets with no diurnal variation. These would influence the capability of the model ability in simulating the spatial and temporal (i.e. diurnal and daily) variations of pollutants in the city.

The seasonal variation of the simulated pollutants' concentration is similar to the observed, except that simulated peak concentration lags the observed peak by two months (Fig. 7). The simulated peak concentrations are in April, while the observed peak concentrations are in June. This

discrepancy may be attributed to the winter rainfall, which cleanses the atmosphere of any accumulated pollutants. Since RegCM underestimates the local emission of the pollutants, the building up of the pollutants in the atmosphere, after the cleansing by the winter rain, may take a longer time in the model than in the observation. The simulated rainfall and temperature show a good agreement with CRU observation, except that the model underestimates temperature in summer months, overestimates rainfall in winter, and underestimates rainfall in winter. However, the model underestimates the concentrations of pollutants in winter (May–August) and overestimates them in other months. The simulated rainfall and temperature show a good agreement with CRU observation, except that the model underestimates temperature in summer months, overestimates rainfall in summer, and underestimates rainfall in winter.

4.3 Characteristics of the simulated pollutant and atmospheric conditions over South Africa

4.3.1 Annual mean

RegCM simulates the hot spots of NO, NO₂ and HNO₃ concentrations over the northeast of South Africa (Fig. 8). The

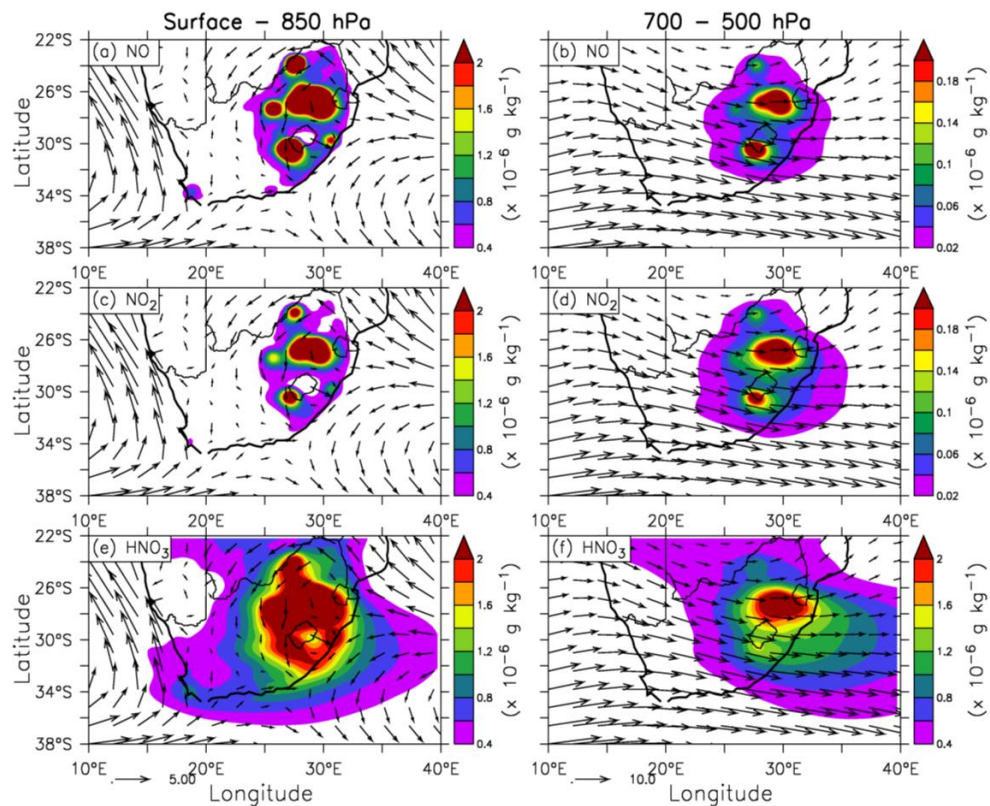


Fig. 8. RegCM4 simulated annual mean (2001–2004) concentration for NO ($\times 10^{-6} \text{ g kg}^{-1}$; top panels), NO₂ ($\times 10^{-6} \text{ g kg}^{-1}$; middle panels) and HNO₃ ($\times 10^{-6} \text{ g kg}^{-1}$; bottom panels) at low level (surface–850 hPa; left panels) and middle level (700–500 hPa; right panels) over South Africa. The corresponding wind speeds are shown with arrows; the arrows at the bottom of the bottom panels (e and f) show the wind scale of 5 m s^{-1} and 10 m s^{-1} , respectively.

maximum concentration of NO (about $30 \times 10^{-6} \text{ g kg}^{-1}$) is over the Mpumalanga Highveld, the area of intense industrial activities in South Africa (Collett et al., 2010). The maximum concentration of NO₂ (about $5.0 \times 10^{-6} \text{ g kg}^{-1}$) is also over the Mpumalanga Highveld, but the magnitude is lower than that of NO, because NO₂ is formed by oxidation of NO (see Eq. 1). The maximum concentration of HNO₃ (about $5.0 \times 10^{-6} \text{ g kg}^{-1}$) is also lower than that of NO, but HNO₃ concentrations cover a wider area than those of NO and NO₂ concentrations. For instance, the contour of $0.5 \times 10^{-6} \text{ g kg}^{-1}$ in HNO₃ covers almost the entire country, but that of NO and NO₂ are limited to the eastern part of the country (Fig. 8). This is because most of the NO and NO₂ are converted to HNO₃ as they are transported away from the hot spots.

The model simulation shows a difference in the transport of the pollutants (NO, NO₂ and HNO₃) at lower level (surface–850 mb) and at upper level (700–500 mb) (Fig. 8). At the upper level (i.e. 700 hPa), the wind pattern is dominated by a westerly flow with a weak trough over the western coast and an anticyclonic flow over the northeast of South Africa. At this level, the westerly flow transports most pollu-

tants from the hot spots towards the Indian Ocean, while the anticyclonic flow recycles the pollutant over southern Africa.

At lower level, the wind pattern is dominated by northerly and northeasterly flows over the continent, southwesterly and southeasterly flows over the Atlantic Ocean, and easterly flows over the Indian Ocean. The northerly and northeasterly flows transport pollutants from the hot spots toward the southern coast and to Cape Town. The northerly flows converge with the southerly winds along the southern coast. The convergence produces weak winds and induces accumulation of the pollutants over the southwestern half of South Africa, along the southern coasts, and over Cape Town. The easterly flow transports fresh air from the Indian Ocean to the eastern coast, but also picks up pollutants from the hot spots and transports them along the coastline towards Cape Town area. Hence, while the upper-level winds (westerlies) transport fresh air eastward from the Atlantic Ocean over the Cape Town area, the surface winds (easterlies and northeasterlies) transport pollutants from the Mpumalanga Highveld toward the city.

The emphases of previous studies have been on the eastward transport of Highveld pollutants by the upper-level westerly flow and on the recirculation of the pollutants over

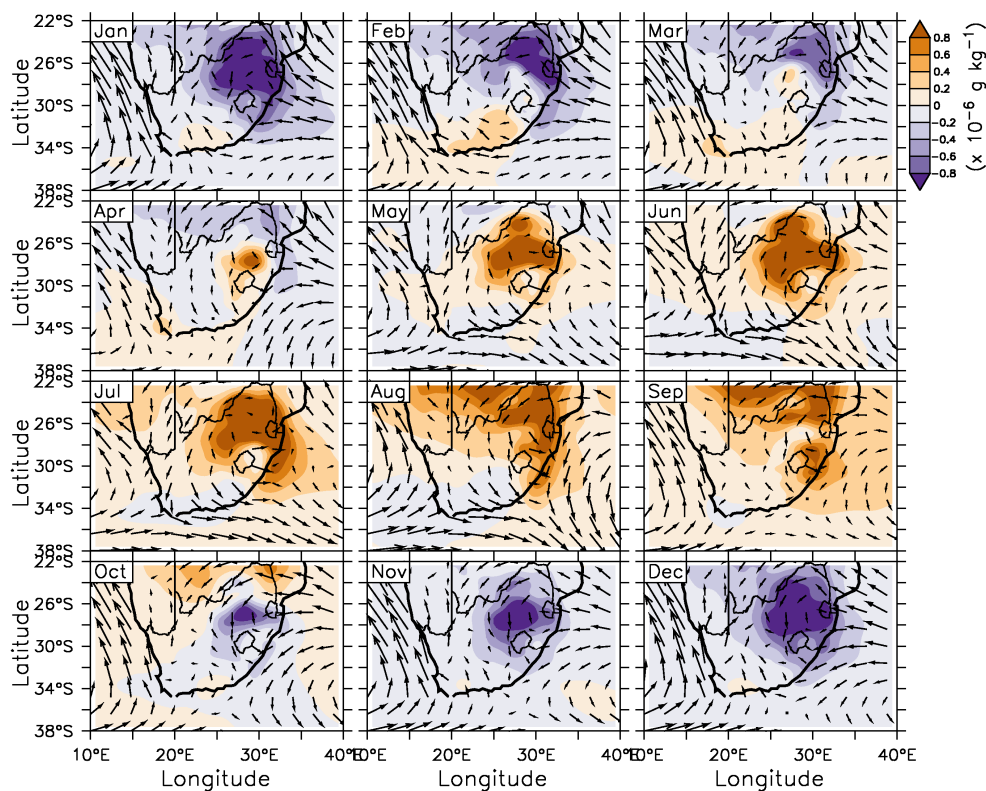


Fig. 9. Monthly anomalies of the simulated HNO_3 concentration ($\times 10^{-6} \text{ g kg}^{-1}$) over South Africa.

southern Africa by the anticyclones. For instance, Freiman and Piketh (2003) show that 39 % of pollutants from the Highveld are transported to the Indian Ocean, 33 % are recycled over the sub-continent, and only 6 % are transported by the northerly flow to the south of the Indian ocean. The present results suggest however that the amount of HNO_3 transported from the Highveld pollutants southward (and towards Cape Town) may be substantial, and given that the winds are weaker at lower level than at upper level, and the pollutant concentrations are higher at low level than at upper level, it is important to have a better understanding of pollutants' transport at low level, especially over South Africa.

Using a high-resolution (about $1.5 \times 1.5 \text{ km}$) simulation over the Western Cape, Jury et al. (1990) attributes the weak wind over the Western Cape to convergence of land and sea breezes; the present study suggests however that the weak wind may be due to convergence of synoptic scale flows, because the lower resolution ($30 \times 30 \text{ km}$) simulation used in the present study cannot resolve land and sea breezes, yet the simulation features the weak wind and further shows that weak wind covers a wider domain than shown in Jury et al. (1990).

4.3.2 Seasonal variation

The simulated HNO_3 over South Africa exhibits a seasonal variability in which atmospheric condition plays a major role (Fig. 9). The highest variability in HNO_3 occurs over the Mpumalanga Highveld, with positive anomalies in April–September and negative anomalies in October–March. The anomalies can be attributed to the prevailing atmospheric conditions during the periods. In summer (October–January), the inversion layer over the eastern coast is elevated above the mountain range (i.e. the escarpment). This allows the easterly flow from the Indian Ocean to penetrate inland and dilute the concentration of HNO_3 over the Mpumalanga Highveld (Fig. 10). The reverse is the case in winter (April–August), when the inversion layer is lower than the peak of the escarpment. The easterly flow cannot penetrate inland with the fresh air; instead, it deflects around the mountain ranges, southward along the coastline or northward toward Mozambique. Rainfall may also lower HNO_3 concentrations in summer, because the eastern part of South Africa experiences intense rainfall in summer and the rainfall will cleanse the atmosphere of HNO_3 .

The seasonal variation of HNO_3 is weaker over Cape Town than over the Mpumalanga Highveld, but the anomalies over Cape Town are substantial and are influenced by transport of HNO_3 from the Mpumalanga Highveld region.

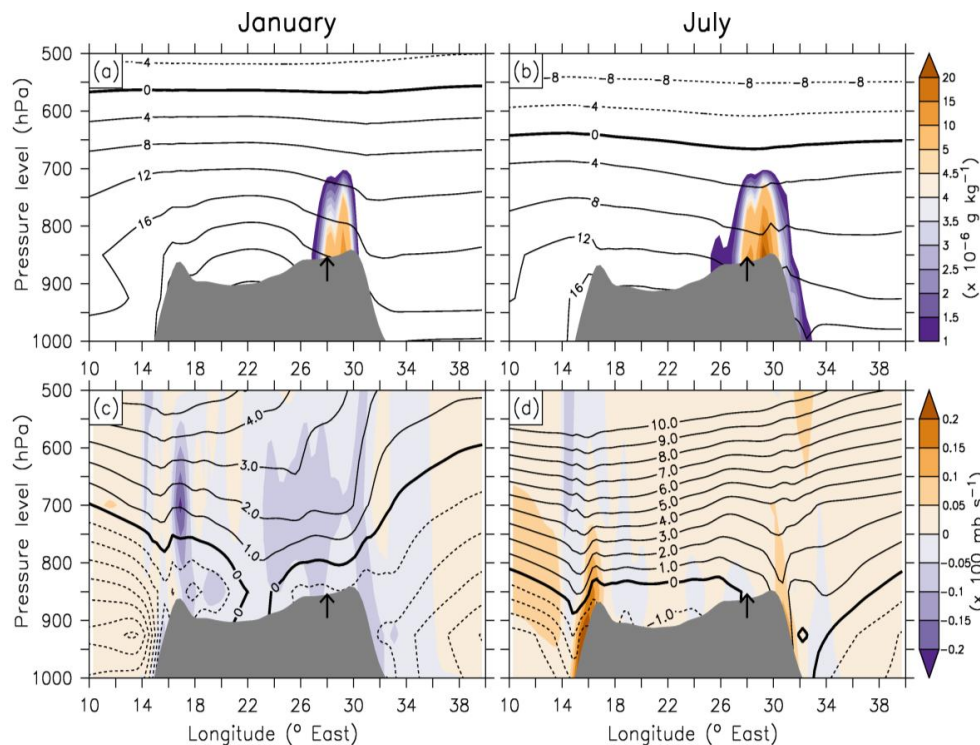


Fig. 10. Vertical cross section of HNO₃ concentration ($\times 10^{-6} \text{ g kg}^{-1}$; shaded in upper panels) and temperature ($^{\circ}\text{C}$; contours in upper panels), vertical wind component ($\times 100 \text{ mb s}^{-1}$; shaded in lower panels), and zonal wind component (m s^{-1} ; contours in lower panels) at latitude 26°S in January and July. Topography is shown in grey colour and the location of the Highveld indicated with the arrow (\uparrow).

The seasonal variability shows strong positive anomalies of HNO₃ in February–April and weaker negative anomalies in other months. The months with the positive anomalies feature easterly and northeasterly flows transporting HNO₃ from the Mpumalanga Highveld toward Cape Town, while the months with negative anomalies are characterized by southwesterly winds transporting fresh maritime air towards Cape Town. Note that, unlike the eastern part of South Africa, Cape Town experiences its intense rainfall in winter. The removal of HNO₃ from the atmosphere by the winter rainfall may contribute to the negative anomalies in winter months.

Table 1 presents the monthly budget of pollutants' (NO, NO₂, NO_x and HNO₃) fluxes over Cape Town at lower level. The monthly mean of the net flux is positive for all the pollutants in each month. That means that, over the city, the magnitude of outgoing pollutants is greater than the magnitude of incoming pollutants; so, Cape Town is a source for the pollutants. For all the pollutants, the maximum net flux occurs in April and the minimum in November, January, or August.

The western boundary of the city always experiences outward fluxes of the pollutants, except in June when it experiences inward fluxes of HNO₃ (Table 1). Its maximum outward flux occurs in January. The northern boundary features inward fluxes for the pollutants in April–August but outward fluxes in the remaining months. The reverse is the case at the southern boundary, where there are outward fluxes in

April–August but inward fluxes in other months. However, in most cases, the magnitudes of the outward fluxes at the western boundary are greater than the magnitude of outward or inward fluxes at other boundaries. Hence, climatologically, Cape Town is a net exporter of the pollutants, and most of the pollutants from the city are exported through the western boundary. However, as it will be shown later, the situation is different during extreme pollution events.

4.3.3 Transport of pollutants during extreme events in Cape Town

The time series of the simulated pollutants' concentration over Cape Town (Fig. 11) shows that the extreme concentration events (defined as 99 percentiles; $\geq 3.3 \times 10^{-6} \text{ g kg}^{-1}$ for NO_x; $\geq 2.8 \times 10^{-6} \text{ g kg}^{-1}$ for HNO₃) mostly occur in April. For NO_x (Fig. 11c), the extreme events occur once in 2001 but twice in 2003 and 2004. For HNO₃, the extreme events occur once 2001, thrice in 2002 and twice in 2003 and 2004. However, the extreme events for NO_x and HNO₃ rarely occur on the same day, suggesting that, in Cape Town, the atmospheric conditions that induce NO_x extreme events may be different from those that induce HNO₃ extreme events. The time difference may also be attributed to the chemical reactions which form HNO₃ from NO_x.

Table 1. The low-level flux budget of pollutants (NO, NO₂, NO_x and HNO₃) over Cape Town for each month, showing the inward and outward fluxes at the western (F_W), eastern (F_E), southern (F_S) and northern (F_N) boundaries of Cape Town and the net flux (F_{Net}) over the city. A positive zonal flux (F_E or F_W) implies a westerly flux (i.e. a flux from a westerly direction), while a negative zonal flux means the opposite. A positive meridional flux (F_N or F_S) denotes a southerly flux (i.e. a flux from a southerly direction), while a negative zonal flux means the opposite. Inward fluxes (from any boundary or direction) into the city are in bold font, while outward fluxes from the city are in thin font. A positive F_{Net} indicates divergence (i.e. depletion) of the pollutants over the city, while a negative net flux means convergence (i.e. accumulation) of the pollutants over the city.

	Jan	Feb	Mar	Apr	May	Jun	Jul	Aug	Sept	Oct	Nov	Dec.
NO												
F_W	-1.9	-2.4	-2.2	-1.3	-0.6	0.0	-0.4	-0.3	-1.1	-1.1	-1.6	-1.7
F_E	-0.4	-1.0	-0.8	0.3	0.5	0.9	0.6	0.9	0.2	0.2	-0.2	-0.4
F_S	1.6	1.5	1.5	-0.4	-0.7	-1.5	-1.2	-0.6	0.3	0.4	1.5	1.4
F_N	1.2	1.0	1.6	-0.2	-0.3	-0.7	-0.6	-0.3	0.1	0.4	1.0	1.2
F_{Net}	1.1	0.9	1.5	1.7	1.5	1.7	1.6	1.5	1.2	1.3	0.9	1.0
NO₂												
F_W	-1.5	-2.0	-1.8	-1.0	-0.5	0.0	-0.4	-0.3	-0.9	-0.9	-1.3	-1.4
F_E	-0.3	-0.6	-0.4	0.2	0.3	0.5	0.3	0.4	0.0	0.1	-0.2	-0.2
F_S	1.2	1.2	1.2	-0.3	-0.5	-1.0	-0.7	-0.4	0.2	0.3	1.1	1.0
F_N	0.8	0.8	1.0	-0.1	-0.2	-0.4	-0.4	-0.2	0.1	0.3	0.7	0.8
F_{Net}	0.9	1.0	1.2	1.4	1.1	1.0	1.0	0.9	0.8	1.0	0.8	0.8
NO_x												
F_W	-3.4	-4.4	-4.0	-2.2	-1.1	-0.1	-0.8	-0.6	-2.0	-2.0	-2.9	-3.0
F_E	-0.7	-1.5	-1.2	0.5	0.8	1.3	1.0	1.3	0.2	0.2	-0.4	-0.6
F_S	2.8	2.7	2.7	-0.7	-1.2	-2.5	-1.9	-1.0	0.5	0.6	2.5	2.5
F_N	1.9	1.8	2.6	-0.3	-0.6	-1.1	-1.0	-0.5	0.2	0.6	1.7	1.9
F_{Net}	1.9	1.9	2.7	3.1	2.6	2.8	2.6	2.3	2.0	2.2	1.7	1.9
HNO₃												
F_W	-3.1	-4.7	-3.7	-1.5	-0.8	0.2	-0.6	-0.5	-2.2	-1.6	-2.6	-2.8
F_E	-1.7	-3.0	-1.6	0.0	0.0	0.6	0.0	0.2	-1.2	-0.7	-1.1	-1.5
F_S	2.8	3.4	3.0	-0.4	-0.7	-1.7	-1.6	-0.7	0.7	0.7	2.5	2.6
F_N	1.8	2.1	2.2	-0.3	-0.6	-1.2	-1.7	-0.6	0.0	0.4	1.6	1.7
F_{Net}	0.4	0.4	1.2	1.6	1.0	0.9	0.6	0.8	0.4	0.6	0.5	0.4

The composite of wind flow during extreme pollution events in Cape Town shows a transport of pollutants from the Mpumalanga Highveld to Cape Town at surface (Fig. 12). For NO_x extreme events, the low-level wind pattern is characterized by northerly and northeasterly flows, transporting the pollutant from the Mpumalanga Highveld towards Cape Town and the south coast.

Along the southern coastline, there is a confluence of the northerly flow and easterly flow; and the easterly flow also transports pollutants from the eastern part of South Africa towards Cape Town. The wind pattern also features a col over Cape Town. A col is a relatively neutral area of low pressure between two anticyclones, or a point of intersection of a trough (in cyclonic flow) and a ridge (in anticyclonic flow). It is usually associated with a calm or light variable wind which causes stagnation of air flow. A col can cause an accumulation of atmospheric pollution (Stein et al., 2003). The formation of a col with the convergence of northeasterly and

southerly flows over Cape Town will provide a favourable atmospheric condition for accumulation of the pollutants over the city during the extreme events.

At 700 hPa (Fig. 13), there is a strong anticyclonic flow over southern Africa. This anticyclone will produce a strong subsidence over South Africa, and the subsidence will prevent a vertical mixing of the pollutants, capping the high concentrations of pollutants close to the surface as they are transported toward from the Mpumalanga Highveld toward Cape Town. The synoptic wind patterns that induce the extreme HNO₃ events differ from those that induce the extreme NO_x events (Fig. 12d). With HNO₃ extreme events, the low-level wind pattern features a strong northwesterly flow transporting HNO₃ from the Mpumalanga Highveld towards the south coast. In addition, it shows a strong easterly flow transporting fresh air from Indian Ocean, but turns poleward as it approaches the escarpment, thereby deflecting the fresh air from the continent, at the same time forming a confluence

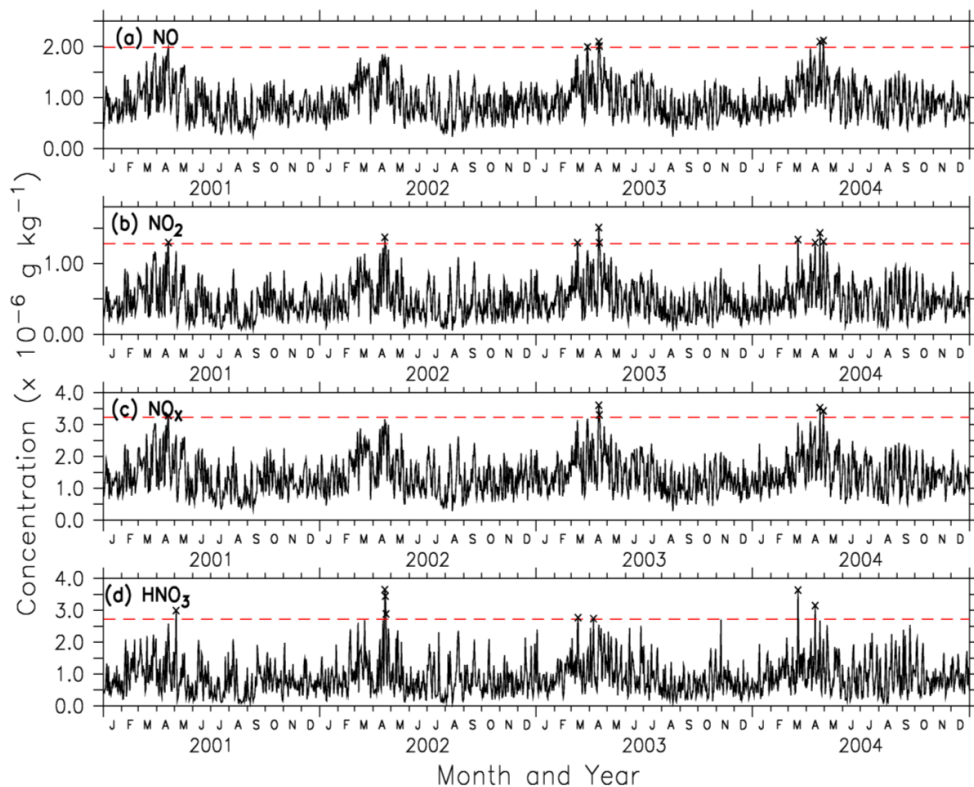


Fig. 11. The time series of the simulated pollutants concentration over Cape Town in 2001–2004. The extreme values (99 percentiles) are indicated with red dashed.

Table 2. The low-level flux budget of pollutants (NO, NO₂, NO_x and HNO₃) during extreme events over Cape Town, showing the inward and outward fluxes at the western (F_W), eastern (F_E), southern (F_S) and northern (F_N) boundaries of Cape Town and the net flux (F_{Net}) over the city. A positive zonal flux (F_E or F_W) implies a westerly flux (i.e. a flux from a westerly direction), while a negative zonal flux means the opposite. A positive meridional flux (F_N or F_S) denotes a southerly flux (i.e. a flux from a southerly direction), while a negative zonal flux means the opposite. Inward fluxes (from any boundary or direction) into the city are in bold font, while outward fluxes from the city are in thin font. A positive F_{Net} indicates divergence (i.e. depletion) of the pollutants over the city, while a negative net flux means convergence (i.e. accumulation) of the pollutants over the city.

	NO		NO ₂		NO _x		HNO ₃		
	March	April	March	April	April	March	April	May	
F_W	−3.1	−0.4	−0.9	−1.0	−0.7	1.4	−0.5	1.0	
F_E	−3.0	−0.7	−0.5	−0.9	−1.4	1.3	0.7	1.1	
F_S	0.8	−0.9	0.5	0.1	−0.8	−0.8	1.8	−0.6	
F_N	−1.1	−2.0	−0.6	−1.1	−1.6	−0.4	0.8	−1.0	
F_{Net}	−1.8	−1.3	−0.7	−1.1	−1.4	0.3	0.2	−0.3	

flow with the northwesterly flow along the coast. The wind patterns also feature a weak wind along the south coast and a col over Cape Town. Hence, there is a band of high HNO₃ concentration along the coast, linking the peak HNO₃ concentration at Cape Town with that over the Mpumalanga Highveld. As with NO_x extreme events, the 700 hPa wind pattern features a strong anticyclone (centering over the border between South Africa and Botswana), but with a stronger northwesterly flow over the western flank of South Africa.

Table 2 shows that Cape Town is a sink for all the pollutants during the extreme events, except for HNO₃ in March and April. For NO_x (NO and NO₂), while the western boundary experiences outward fluxes, the eastern and northern boundaries experience inward fluxes with higher magnitudes than the outward fluxes at the western boundary. The direction of the fluxes at the southern boundary varies: inward fluxes for NO in March, NO₂ in March and April, but outward fluxes for NO and NO_x in April. Nevertheless, net

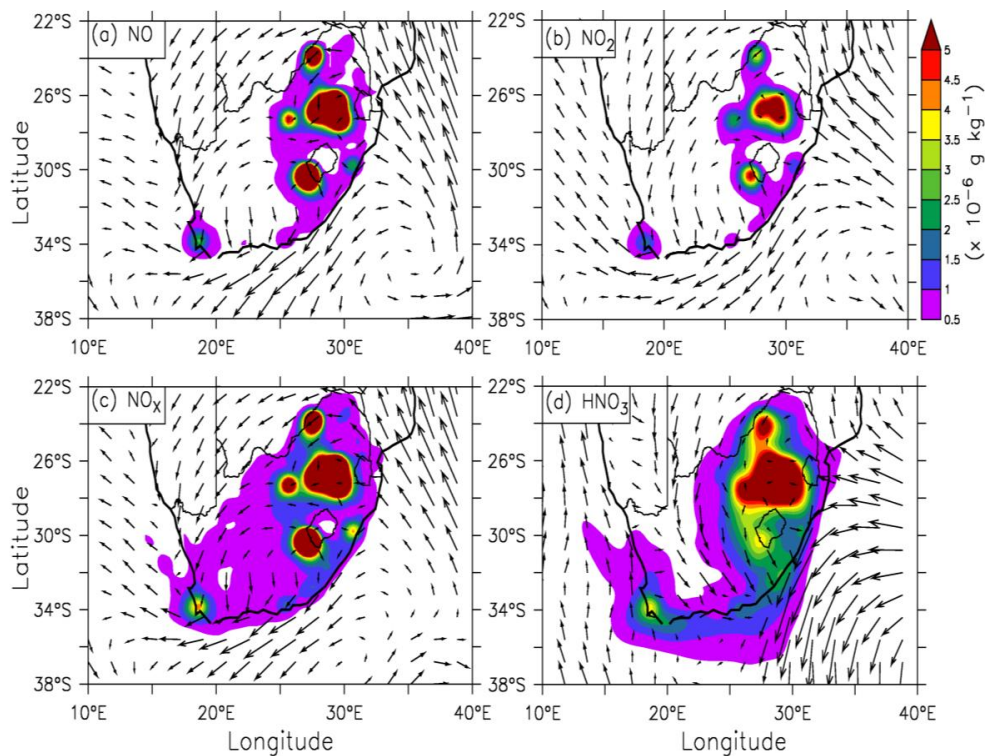


Fig. 12. The composite of low-level (surface–850 hPa) wind flow (arrow) during the extreme pollution events in Cape Town. The corresponding pollutant concentrations (NO, NO₂, NO_x and HNO₃; $\times 10^{-6} \text{ g kg}^{-1}$) are shaded.

fluxes for NO_x (NO and NO₂) are negative, meaning accumulation of NO_x (NO and NO₂) over the city, during the extreme event.

The characteristics of HNO₃ fluxes during the extreme events differ from (and are more complex than) those of NO_x. For HNO₃, the western and northern boundaries experience inward fluxes during the extreme events in March and May but outward fluxes in April. The eastern boundary experiences outward fluxes of HNO₃, while the southern boundary experiences inward fluxes in April but outward fluxes in March and May. Nevertheless, the table indicates an accumulation of HNO₃ over Cape Town in May, though not in March and April.

5 Conclusion

As part of ongoing efforts to understand the sources of pollution in Cape Town, this study has applied a regional climate model (RegCM) to study the transport of NO_x and HNO₃ over South Africa, with emphasis on pollutants transported from the Mpumalanga Highveld to Cape Town. It also examines whether Cape Town is a net sink or source for the pollutants. The model accounts for the influence of southern African complex topography, atmospheric conditions and pollutant chemical reactions in simulating the emission, dispersion and transport of the pollutants. The study described

the characteristic of observed NO and NO₂ over Cape Town, examined how well the regional model captures the characteristics, and analysed the model simulations to describe the influence of atmospheric conditions on the seasonal variations of the pollutants over South Africa. It calculated the flux budget of the pollutant over the city for each month and for composite of days with extreme pollution events.

The diurnal variation of NO_x over Cape Town exhibits two peaks (morning and evening peak) mainly owing to traffic rush, but the atmospheric conditions also play a critical role on the morning peak. The seasonal variation is more influenced by changes in the atmospheric conditions than changes in the local emissions from traffic or industries. The model shows some biases in simulating the seasonal variation of NO_x (NO and NO₂) concentration as observed. The simulated peak concentrations lag the observed peak by two months; the simulated peak concentrations are in April while the observed peak concentrations are in June. The correlation coefficient between the observed and simulated daily concentration of the pollutants is about 0.4, while the normalized standard deviation varies between 0.4 and 1.0. However, the model performs better in simulating the atmospheric variables.

While the results of this study agree with those from previous studies that the Mpumalanga Highveld's pollutants are transported eastward by the westerly flow at 700 hPa,

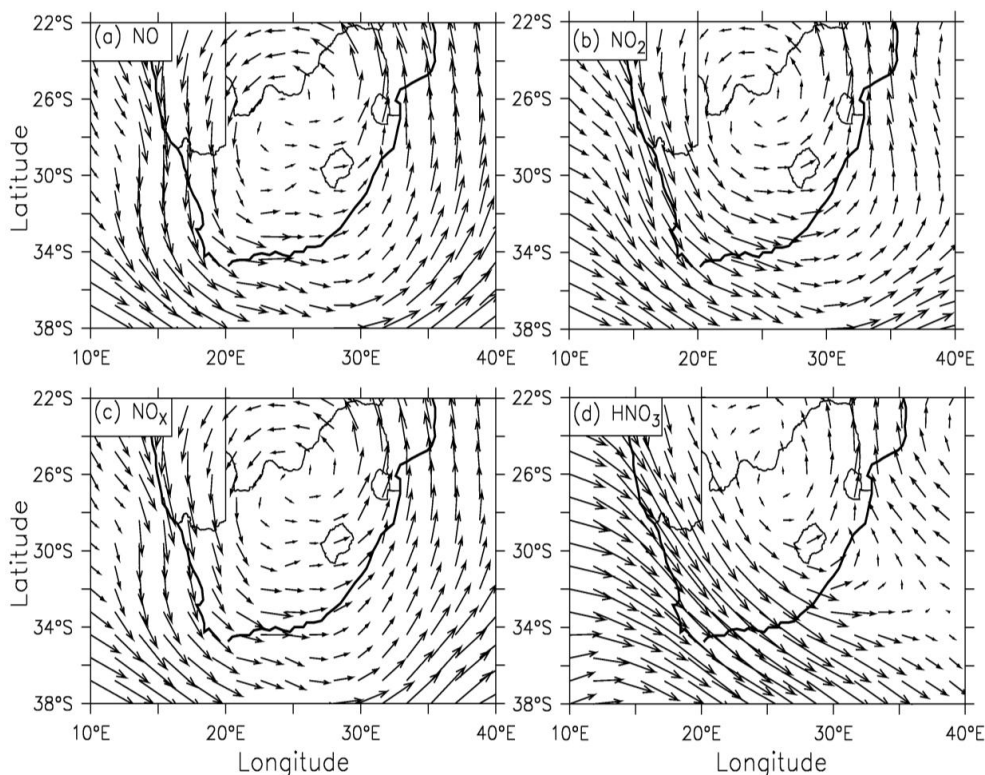


Fig. 13. The composite of 700 hPa wind flow during extreme events of pollutants (NO, NO₂, NO_x and HNO₃) concentration at surface in Cape Town.

they show that the reverse is the case at low level (surface–850 hPa), where the concentration of the pollutant is higher. At the low level, the easterly and northeasterly flows transport the Mpumalanga Highveld's pollutants westward toward Cape Town, and during the extreme events, the northeasterly flow transports NO_x directly from the Mpumalanga Highveld to Cape Town. A band of high concentration of HNO₃ links the peak HNO₃ concentration at Cape Town with that of the Mpumalanga Highveld, and the 700 hPa synoptic winds feature a strong anticyclone that induces strong subsidence over South Africa. The formation of a col over Cape Town during the extreme event makes conditions conducive for accumulation of pollutants. However, the pollutants' budget flux over Cape Town shows that the city could be a net source or net sink for NO_x and HNO₃ during the extreme events.

Since the seasonal peak of the simulated pollutant occurs in April instead of June, and these two months have different seasonal wind patterns, the simulated wind patterns and pollutant transports the model associates with the simulated extreme events in June may not be applicable to the observed extreme events in August. Hence, further studies are needed to investigate the role of regional atmospheric conditions and pollutant transports on the extreme pollution events in August. However, enhanced observations of HNO₃ would be valuable to future investigations and validation. In

addition, since the results of the present study are based on four years of simulation from one model, there is need for longer simulations with multi-models to establish the robustness of the findings. A longer simulation will account for the influence of inter-annual variability on the results, while using multi-model simulations will provide opportunity for the comparison of models and for assessing the degree of inter-model variability. However, the present study suggests that the transport of NO_x and HNO₃ from the Mpumalanga Highveld may contribute to the pollutants' concentration in Cape Town.

Acknowledgements. The project was supported with grants from the National Research Foundation (NRF, South Africa) and the Applied Centre for Climate and Earth Sciences (ACCESS). The third author was supported with grants from the African Centre for Cities (ACC). Computations facility was provided by the Centre for High Performance Computing (CHPC, South Africa). We thank the anonymous reviewers, whose comments improved the quality of this manuscript.

Edited by: M. Palm

References

- Bravo, A. H., Soto, A. R., Sosa, E. R., Sánchez, A. P., Alarcón, J. A. L., Kahl, J., and Ruíz, B. J.: Effect of acid rain on building material of the El Tajín archaeological zone in Veracruz, Mexico, *Environ. Pollut.*, 144, 655–660, 2006.
- Cheng, R. J., Hwu, J. R., Kim, J. T., and Leu, S. M.: Deterioration of Marble Structures The Role of Acid Rain. *Anal. Chem.*, 59, 104A–106A, 1987.
- City of Cape Town: Air Quality Management Plan for the City of Cape Town, Cape Town, 2005.
- Collett, K. S., Piketh, S. J., and Ross, K. E.: An assessment of the atmospheric nitrogen budget on the South African Highveld, *South Afr. J. Sci.*, 106, 1–9, 2010.
- Dean, A. M. and Bozzelli, J. W.: Combustion Chemistry of Nitrogen In: Gas-Phase Combustion Chemistry, Edited by: ardiner Jr., W. C., Springer Link pg. 1 – 123, ISBN: 978-1-4612-7088-1 (Print) 978-1-4612-1310-9 (Online), 2000.
- Dean, S. W.: Corrosion testing of metals under natural atmospheric conditions. In *Corrosion Testing and Evaluation*, Silver Anniversary Volume, Philadelphia, PA, ASTM, 163–76, 1990.
- Dickinson, R. E., Henderson-Sellers, A. and Kennedy, P. J.: Biosphere-atmosphere transfer scheme (BATS) version 1e as coupled to the NCAR community climate model, Technical report, Boulder, Colorado, 1993.
- Emmons, L. K., Walters, S., Hess, P. G., Lamarque, J.-F., Pfister, G. G., Fillmore, D., Granier, C., Guenther, A., Kinnison, D., Laepple, T., Orlando, J., Tie, X., Tyndall, G., Wiedinmyer, C., Baugcum, S. L., and Kloster, S.: Description and evaluation of the Model for Ozone and Related chemical Tracers, version 4 (MOZART-4), *Geosci. Model Dev.*, 3, 43–67, doi:10.5194/gmd-3-43-2010, 2010.
- Fields, S.: Cycling out of Control, *Environ. Health Perspect.*, 112, 556–563, 2004.
- Freiman, M. T. and Piketh, S. J.: Air transport into and out of the industrial Highveld region of South Africa, *J. Appl. Meteorol.*, 42, 994–1002, 2003.
- Fritsch, J. M. and Chappell, C. F.: Numerical prediction of convectively driven mesoscale pressure systems, Part I: Convective parameterization, *J. Atmos. Sci.*, 37, 1722–1733, 1980.
- Gauderman, W. J., McConnell, R. O. B., Gilliland, F., London, S., Thomas, D., Avol, E., and Peters, J.: Association between air pollution and lung function growth in southern California children, *Am. J. Resp. Crit. Care Med.*, 162, 1383–1390, 2000.
- Giorgi, F. and Anyah, R. O.: The Road Towards RegCM4., *Clim. Res.*, 52, 3–6, 2012.
- Grell, G. A., Peckham, S. E., Schmitz, R., McKeen, S. A., Frost, G., Skamarock, W. C., and Eder, B.: Fully coupled online chemistry within the WRF model, *Atmos. Environ.*, 39, 6957–6975, 2005.
- Holtslag, A. A. M. and Boville, B. A.: Local versus nonlocal boundary-layer diffusion in a global climate model, *J. Climate*, 6, 1825–1842, 1993.
- Jury, M., Tegen, A., Ngeleza, E., and Dutoit, M.: Winter air pollution episodes over Cape Town, *Bound.-Layer Meteorol.*, 53, 1–20, 1990.
- Kiehl, J. T., Hack, J. J., Bonan, G. B., Boville, B. A., Briegleb, B. P., Williamson, D. L., and Rasch, P. J.: Description of the NCAR community climate model (CCM3), Technical report NCAR/TN-420+STR, Boulder, Colorado, 1996.
- Likens, G. E. and Bormann, F. H.: Acid rain: a serious regional environmental problem. *Science*, 184, 1176–1179, 1974.
- Madronich, S. and Flocke, S.: The role of solar radiation in atmospheric chemistry., edited by: Boule, P., in: *Handbook of Environmental Chemistry*, New York, Springer-Verlag, 1–26, 1999.
- Minns C. K., Kelso, J. R. M., and Johnson, M. G.: Large-Scale Risk Assessment of Acid Rain Impacts on Fisheries: Models and Lessons, *Canad. J. Fish. Aquat. Sci.*, 43, 900–921, doi:10.1139/f86-113, 1986.
- Mitchell, T. D. and Jones, P. D.: An Improved Method of Constructing a Database of Monthly Climate Observations and Associated High-resolution grids, *Int. J. Clim.*, 25, 693–712, 2005.
- Monin, A. S. and Obukhov, A. M.: Osnovnye zakonomernosti turbulentnogo peremesivaniya v prizemnom sloc atmosfery y (Basic laws of turbulent mixing in the atmosphere near the ground), *Trudy Institute Geologicheskikh Geofizi*, 24, 163–187, 1954.
- Moss, R. H., Edmonds, J. A., Hibbard, K. A., Manning, M. R., Rose, S. K., van Vuuren, D. P., Carter, T. R., Emori, S., Kainuma, M., Kram, T., Meehl, G. A., Mitchell, J. F. B., Nakicenovic, N., Riahi, K., Smith, S. J., Stouffer, R. J., Thomson, A. M., Weyant, J. P., and Wilbanks, T. J.: The next generation of scenarios for climate change research and assessment, *Nature*, 463, 747–756, doi:10.1038/nature08823, 2010.
- Ostro, B. D., Lipsett, M. J., Wiener, M. B., and Selner, J. C.: Asthmatic responses to airborne acid aerosols, *Am. J. Publ. Health*, 81, 694–702, 1991.
- Pal, J. S., Giorgi, F., Bi, X., Elguindi, N., Solmon, F., Gao, X., Francisco, R., Zakey A., Winter, J., Ashfaq, M., Syed, F. S., Sloan, L. C., Bell, J. L., Diffenbaugh, N. S., Karmacharya, J., Konaré, A., Martinez, D., da Rocha, R. P., and Steiner, A. L.: Regional Climate Modeling for the Developing World: The ICTP RegCM3 and RegCNET, *B. Am. Meteorol. Soc.*, 88, 1395–1409, 2007.
- Piketh, S. J., Swap, R. J., Maenhaut, W., Annegarn, H. J., and Formenti, P.: Chemical evidence of long-range atmospheric transport over southern Africa, *J. Geophys. Res.*, 107, 1–13, 2002.
- Preston-Whyte, R. A., Diab, R. D., and Tyson, P. D.: Towards an inversion climatology of southern Africa, II, Non-surface inversions in the lower atmosphere, *South Afr. Geogr. J.*, 59, 47–59, 1977.
- Samie, F., Tidblad, J., Kucera, V., and Leygraf, C.: Atmospheric corrosion effects of HNO₃ – a comparison of laboratory-exposed copper, zinc and carbon steel. *Atmos. Environ.*, 41, 4888–4896 2007.
- Sander, S. P., Abbatt, J., Barker, J. R., Burkholder, J. B., Friedl, R. R., Golden, D. M., Huie, R. E., Kolb, C. E., Kurylo, M. J., Moortgat, G. K., Orkin, V. L., and Wine, P. H.: Chemical Kinetics and Photochemical Data for Use in Atmospheric Studies, Evaluation No. 17, JPL Publication 10-6, Jet Propulsion Laboratory, Pasadena, <http://jpldataeval.jpl.nasa.gov>, 2011.
- Schulz, U., Trubiroha, P., Schernau, U., and Baumgart, H.: The effects of acid rain on the appearance of automotive paint systems studied outdoors and in a new artificial weathering test, *Progress in organic coatings*, 40, 151–165, 2000.
- Schuster, P. F., Reddy, M. M., and Sherwood, S. I.: Effects of acid rain and sulfur dioxide on marble dissolution, *Mat. Perform.*, 33, 76–80, 1994.
- Schwartz, J. and Marcus, A.: Motility and air pollution in London: a time-series analysis, *Am. J. Epidemiol.*, 131 185–194, 1990.

- Seinfeld, J. H. and Pandis, S. N.: Atmospheric Chemistry and Physics: From Air Pollution to Climate Change, 2nd edition, J. Wiley, New York, 1203 pp., 2006.
- Shalaby, A., Zakey, A. S., Tawfik, A. B., Solmon, F., Giorgi, F., Stordal, F., Sillman, S., Zaveri, R. A., and Steiner, A. L.: Implementation and evaluation of online gas-phase chemistry within a regional climate model (RegCM-CHEM4), *Geosci. Model Dev.*, 5, 741–760, doi:10.5194/gmd-5-741-2012, 2012.
- StatsSA 2012: Cape Town Profile, Cape Town: Statistics South Africa, http://www.capetown.gov.za/en/stats/Documents/2011%20Census/2011_Census_Cape_Town_Profile.pdf (last access: 9 January, 2014), 2012.
- Stein, D. C., Swap, R. J., Greco, S., Piketh, S. J., Macko, S. A., Doddridge, B. G., Elias, T., and Bruintjes, R. T.: Haze Layer Characterization and Associated Meteorological Controls Along the Eastern Coastal Region of Southern Africa, *J. Geophys. Res.*, 108, 1–11, 2003.
- Stern, F. B., Halperin, W. E., Hornung, R. W., Ringenburg, V. L., and Mccammon, C. S.: Heart disease mortality among bridge and tunnel officers exposed to carbon monoxide, *Am. J. Epid.*, 128, 1276–1288, 1988.
- Sylla, M. B., Coppola, E., Mariotti, L., Giorgi, F., Ruti, P. M., Dell'Aquila, A., and Bi, X.: Multiyear simulation of the African climate using a regional climate model (RegCM3) with the high resolution ERA-interim reanalysis, *Clim. Dynam.*, 35, 231–247, 2009.
- van Vuuren, D., Edmonds, J., Kainuma, M., Riahi, K., Thomson, A., Hibbard, K., Hurtt, G., Kram, T., Krey, V., Lamarque, J. F., Masui, T., Meinshausen, M., Nakicenovic, N., Smith, S., and Rose, S.: The representative concentration pathways: an overview, *Clim. Change*, 109, 5–31, 2011.
- Walton, N. M.: Characterisation of Cape Town Brown Haze. University of the Witwatersrand, Johannesburg, 2005.
- Welburn, A.: Air pollution and acid rain: the biological impact. Longman Scientific and Technical, 1988.
- Wesley, M. L.: Parameterization of surface resistance to gaseous dry deposition in regional-scale numerical models, *Atmos. Environ.*, 23, 1293–1304, 1989.
- Wicking-Baird, M. C., De Villiers, M. G. and Dutkiewicz, R.: Cape Town Brown Haze Study, Report No. Gen 192, Cape Town, 1997.
- Yang, W. and Omaye, S. T.: Air pollutants, oxidative stress and human health, *Mutation Research/Genetic Toxicology and Environmental Mutagenesis*, 674, 45–54, 2009.
- Zaveri, R. A. and Peters, L. K.: A new lumped structure photochemical mechanism for long-scale applications, *J. Geophys. Res.*, 30, 387–415, 1999.